FEED-FORWARD CONTROL OF A PRE-CRACKED CANTILEVER BEAM

Sudhir KAUL[1]

This paper develops two feed-forward control algorithms in order to mitigate crack propagation in a cantilever beam with a pre-existing crack. The main objective of the control algorithms is to minimize or reduce transverse deflection at the crack location so as to contain the damage resulting from the pre-existing crack and, thereby, reduce the rate of crack propagation. A point-load sinusoidal excitation, from a known disturbance, is used as the input load acting on the beam. Two control algorithms are used – the first control algorithm computes a control force to eliminate transverse displacement at the crack location resulting from the excitation force, and the second control algorithm minimizes the mean square transverse displacement over a section of the beam that contains the crack. Both the control algorithms are non-causal and assume that the excitation input is completely known a priori. Simulation results for a cantilever beam are presented and discussed in detail. It is observed that the rate of crack propagation can be significantly reduced by implementing the proposed feed-forward control algorithms, increasing the useful life of the damaged beam. Also, it is found that the transverse displacement over a significant length of the beam can be substantially reduced when the beam response is dominated by a specific mode.

Keywords: Feed-forward Control, Beam, Crack.

1. Introduction

Active control of structures is an established area of research that encompasses aspects of structural dynamics, theory of vibrations and active control, and has been thoroughly studied over the last four decades. Housner et al. [1] presented an extensive survey of existing literature in structural control, listing theoretical and experimental advances made in multiple aspects of the subject matter with a summary of possible future research areas of structural control. Alkhatib and Golnaraghi [2] presented an updated review on the status of research in active structural control with a brief listing of associated issues. Meirovitch [3] and Soong [4] presented a theoretical framework of the subject, compiled extensive bibliographies and listed issues associated with structural control such as spillover, time delay, modeling errors and controller and sensor locations.

[1] Senior Lecturer, University of Pretoria, South Africa, E-mail: sudhir.kaul@up.ac.za

Feed-forward control has been found to be preferable in some applications for disturbance rejection [2, 5, 6], where the disturbance is limited to a single frequency or a limited number of multiple frequencies. The feed-forward algorithms implemented in this paper assume a known excitation (or disturbance) frequency and use the a priori information to mitigate damage in a pre-cracked beam, which can be relevant to disturbance rejection applications [5].

The dynamics of cracked structures has been studied theoretically and experimentally by researchers in order to understand the influence of crack growth on dynamic properties of damaged structures. The core motivation of this research has been to develop an understanding of the dynamics of cracked structures in order to predict or detect structural damage by monitoring dynamic properties, like natural frequencies, damping ratios and mode shapes of the cracked structure or by analyzing frequency response of the damaged structure. Dimarogonas [7] presented a comprehensive literature review in the study of cracked structures. Analytical, numerical and experimental results available till mid-1990s were summarized and the areas of study that still need further investigation were listed. Salawu [8] reviewed the methods that have been used by researchers to assess structural damage by tracking the natural frequency of a cracked structure. Some limitations of using natural frequency as the only diagnostic parameter for detecting structural damage were also listed. Shih and Wu [9] studied the relationship between crack propagation of a straight, edge-crack in a rectangular plate and the transverse vibration input. It was concluded that the vibrating frequency has a significant influence on the rate of crack growth. Chasalevris and Papadopoulos [10] used the wavelet transform in order to identify cracks on a beam with two transverse cracks. The identification technique yielded crack depth, crack location as well as crack orientation. Lee and Shin [11] proposed a damage identification method by using a frequency response function-based technique. The technique was demonstrated on beam structures with positive results. Lee [12] proposed an alternative method for identification of cracks in a simply supported beam by using the boundary element method instead of the more commonly used method of using a rotational spring to model the crack. Chondros et al. [13] used the continuous cracked beam theory to model single-edge and double-edge cracks in beams. The model showed strong correlation with experimental results.

This paper proposes the use of feed-forward control algorithms in order to mitigate crack propagation, thereby demonstrating active structural control of a damaged structure by using a cantilever beam as a specimen. The methodology presented in this work combines aspects of fracture mechanics, structural dynamics and active control, which integrates the advances made in three distinct but interrelated areas of research. Though the model and the control algorithms discussed in this paper have been developed specifically for a cantilever beam, a

similar approach may be adopted for any other structure with known dynamics and an already identified damage.

This paper has been divided into four sections. Section 2 develops the model of the cantilever beam with a transverse crack. Section 3 discusses the development of control algorithms in order to limit or eliminate transverse deflection at the crack location. Section 4 presents the simulation results and Section 5 draws overall conclusions.

2. Modeling

This section presents the governing equation of motion (EOM) for the cantilever beam with a single transverse crack. The forced response of the cracked beam is developed in terms of the first three natural modes of the beam.

Using the Euler-Bernoulli model of a beam, the governing EOM for a beam with a constant area of cross-section, A, and a time varying force acting on the beam can be expressed as follows:

$$\rho A\frac{\partial^2}{\partial t^2}y(x,t)+EI\left[\alpha_1+\alpha_2\left(1+Cos\omega t\right)\right]\frac{\partial^4}{\partial x^4}y(x,t)=f_s(x,t) \tag{1}$$

In Eq. (1), E is the modulus of elasticity of the beam material, ρ is the density of the beam material and I is the area moment of inertia of the cross-section. $y(x,t)$ is the transverse displacement of the beam and f_s (x, t) is the time varying force per unit length acting as the excitation load on the beam. Further, α_1 and α_2 are constants used to model the transverse crack as completely open or an opening and closing crack, called as a breathing crack in the literature [14], with the breathing frequency being equal to the excitation frequency, ω. This paper assumes an open crack with $\alpha_1 = 1$ and $\alpha_2 = 0$. The homogeneous or free vibration solution is determined by ignoring the forcing function. The homogeneous form of Eq. (1) can be written as follows:

$$\frac{\partial^2}{\partial t^2}y(x,t)+c^2\frac{\partial^4}{\partial x^4}y(x,t)=0 \tag{2}$$

In Eq. (2), $c^2=\dfrac{EI}{\rho A}$. The homogeneous solution can be obtained by using separation of variables and substituting $y(x,t)=X(x)T(t)$ in Eq. (2). This yields two ordinary differential equations (ODE) which can be solved for $X(x)$ and $T(t)$ separately. The two equations can be expressed as:

$$\frac{d^4}{dx^4}X(x) - \beta^4 X(x) = 0$$
$$\frac{d^2}{dt^2}T(t) + \omega^2 T(t) = 0 \tag{3}$$

In Eq. (3), β is a constant and is defined as follows:

$$\beta^4 = \frac{\omega^2}{c^2} = \frac{\rho A \omega^2}{EI} \tag{4}$$

In Eq. (4), ω is a constant that couples the two differential equations in Eq. (3). The solution of the ODE in Eq. (3) can be expressed as:

$$X(x) = C\,Cos\beta x + D\,Sin\beta x + E\,Cosh\beta x + F\,Sinh\beta x$$
$$T(t) = A Cos\omega t + B Sin\omega t \tag{5}$$

In Eq. (5), *C*, *D*, *E*, *F* are constants that can be determined from the substitution of the boundary conditions and *A*, *B* are constants that can be determined from the substitution of the initial conditions.

The most commonly used model for a cracked beam consists of a torsional spring at the crack location that represents the crack [15, 16, 17], with the stiffness of the spring depending on the geometry of the crack and the overall beam parameters. The computation of the spring stiffness is based on the use of Castigliano's theorem and is shown in Appendix A for an open single-sided edge-crack in a cantilever beam, as shown in Fig. 1. This formulation allows for the solution in Eq. (5) to be re-written as:

$$X_1(x) = X(x) = c_1 Cos\beta x + c_2 Sin\beta x + c_3 Cosh\beta x + c_4 Sinh\beta x \quad for \quad 0 \le x < l_1$$
$$X_2(x) = X(x) = c_5 Cos\beta x + c_6 Sin\beta x + c_7 Cosh\beta x + c_8 Sinh\beta x \quad for \quad l_1 \le x \le l \tag{6}$$
$$T(t) = A Cos\omega t + B Sin\omega t$$

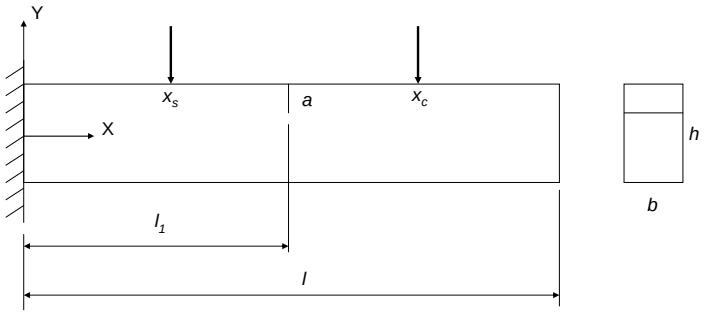

Fig. 1. Pre-cracked Cantilever Beam

In Eq. (6), c_1, …, c_8 are constants determined by incorporation of boundary conditions as well as compatibility conditions associated with the torsional spring modeled at the crack location. The compatibility conditions ensure that the

displacement, the bending moment and the shear force are identical on the two sides of the crack. Additionally, the angular displacement between the two segments of the beam is coupled with the flexibility of the torsional spring used to represent the crack. The boundary conditions and the compatibility conditions are as follows:

$$\begin{aligned} y(0,t) &= \left.\frac{\partial y(x,t)}{\partial x}\right|_{x=0} = 0 \\ \left.\frac{\partial^2 y(x,t)}{\partial x^2}\right|_{x=l} &= \left.\frac{\partial^3 y(x,t)}{\partial x^3}\right|_{x=l} = 0 \\ X_1(l_1) &= X_2(l_1) \\ X_1''(l_1) &= X_2''(l_1) \\ X_1'''(l_1) &= X_2'''(l_1) \\ X_2'(l_1) - X_1'(l_1) &= \theta l\, X_2''(l_1) \end{aligned} \tag{7}$$

In Eq. (7), l is the length of the beam, l_1 indicates the location of the crack, as well as the modeled spring, and θ is the non-dimensional compliance of the torsional spring used to model the crack, as derived in the Appendix A. The first two conditions in Eq. (7) are the boundary conditions associated with the two ends of the cantilever beam and the next four conditions represent the compatibility conditions between the two ends of the beam with the crack in between.

Substitution of all the boundary conditions and compatibility conditions in the solution from Eq. (6) yields the governing frequency equation of the cantilever beam with a single transverse crack as:

$$\det(\Delta) = 0 \tag{8}$$

Eq. (8) is the frequency equation and yields multiple solutions, β_n, for n = 1, 2, …, yielding the corresponding natural frequencies, ω_n, using Eq. (4). Eq. (8) represents the determinant of Δ, which is a function of crack location, l_1, and compliance of the torsional spring, θ, which in turn is a function of the crack size, a, and is defined as follows:

$$\Delta = \begin{bmatrix} 0 & 0 & -C_{\beta_n l} & -S_{\beta_n l} & Ch_{\beta_n l} & Sh_{\beta_n l} \\ 0 & 0 & S_{\beta_n l} & -C_{\beta_n l} & Sh_{\beta_n l} & Ch_{\beta_n l} \\ C_{\beta_n l_1} - Ch_{\beta_n l_1} & S_{\beta_n l_1} - Sh_{\beta_n l_1} & -C_{\beta_n l_1} & -S_{\beta_n l_1} & -Ch_{\beta_n l_1} & -Sh_{\beta_n l_1} \\ -C_{\beta_n l_1} - Ch_{\beta_n l_1} & -S_{\beta_n l_1} - Sh_{\beta_n l_1} & C_{\beta_n l_1} & S_{\beta_n l_1} & -Ch_{\beta_n l_1} & -Sh_{\beta_n l_1} \\ S_{\beta_n l_1} - Sh_{\beta_n l_1} & -C_{\beta_n l_1} - Ch_{\beta_n l_1} & -S_{\beta_n l_1} & C_{\beta_n l_1} & -Sh_{\beta_n l_1} & -Ch_{\beta_n l_1} \\ S_{\beta_n l_1} + Sh_{\beta_n l_1} & -C_{\beta_n l_1} + Ch_{\beta_n l_1} & -S_{\beta_n l_1} + \theta l \beta_n C_{\beta_n l_1} & C_{\beta_n l_1} + \theta l \beta_n S_{\beta_n l_1} & Sh_{\beta_n l_1} - \theta l \beta_n Ch_{\beta_n l_1} & Ch_{\beta_n l_1} - \theta l \beta_n Sh_{\beta_n l_1} \end{bmatrix} \tag{9}$$

In Eq. (9), *S, C, Sh* and *Ch* are used to represent the sine, cosine, sine-hyperbolic and cosine-hyperbolic functions respectively with their arguments written as subscripts.

Substituting the solution of Eq. (8) and the conditions from Eq. (7) in Eq. (6) yields $c_3 = -c_1$ and $c_4 = -c_2$, and arbitrarily substituting $c_1 = 1$, yields the remaining constants in the form of a matrix solution as:

$$\begin{bmatrix} c_{2n} \\ c_{5n} \\ c_{6n} \\ c_{7n} \\ c_{8n} \end{bmatrix} = F^{-1}\left(\beta_n l, l_1, \theta\right) \begin{bmatrix} 0 \\ Ch_{\beta_n l_1} - C_{\beta_n l_1} \\ Ch_{\beta_n l_1} + C_{\beta_n l_1} \\ Sh_{\beta_n l_1} - S_{\beta_n l_1} \\ -S_{\beta_n l_1} - Sh_{\beta_n l_1} \end{bmatrix} \tag{10}$$

In Eq. (10), subscript '*n*' has been added to the constants since the constants vary with the corresponding value of β_n, as determined from Eq. (8). The right hand side of Eq. (10) is a function of $\beta_n l$, the dimensionless compliance of the torsional spring used to model the crack and the crack location with the function, *F*, defined as follows:

$$F\left(\beta_n l, l_1, \theta\right) = \begin{bmatrix} 0 & S_{\beta_n l} & -C_{\beta_n l} & Sh_{\beta_n l} & Ch_{\beta_n l} \\ S_{\beta_n l_1} - Sh_{\beta_n l_1} & -C_{\beta_n l_1} & -S_{\beta_n l_1} & -Ch_{\beta_n l_1} & -Sh_{\beta_n l_1} \\ -S_{\beta_n l_1} - Sh_{\beta_n l_1} & C_{\beta_n l_1} & S_{\beta_n l_1} & -Ch_{\beta_n l_1} & -Sh_{\beta_n l_1} \\ -C_{\beta_n l_1} - Ch_{\beta_n l_1} & -S_{\beta_n l_1} & C_{\beta_n l_1} & -Sh_{\beta_n l_1} & -Ch_{\beta_n l_1} \\ -C_{\beta_n l_1} + Ch_{\beta_n l_1} & -S_{\beta_n l_1} + \theta l \beta_n C_{\beta_n l_1} & C_{\beta_n l_1} + \theta l \beta_n S_{\beta_n l_1} & Sh_{\beta_n l_1} - \theta l \beta_n Ch_{\beta_n l_1} & Ch_{\beta_n l_1} - \theta l \beta_n Sh_{\beta_n l_1} \end{bmatrix} \tag{11}$$

The solutions from Eqs. (8) and (10) yield the mode shapes of the cantilever beam with a single edge-crack as:

$$X_n\left(x\right) = \begin{cases} c_{2n}\left(Sin\beta_n x - Sinh\beta_n x\right) + \left(Cos\beta_n x - Cosh\beta_n x\right) & for \quad 0 \le x < l_1 \\ c_{5n} Cos\beta_n x + c_{6n} Sin\beta_n x + c_{7n} Cosh\beta_n x + c_{8n} Sinh\beta_n x & for \quad l_1 \le x \le l \end{cases} \tag{12}$$

The complete solution for the homogeneous system in Eq. (2) can be now expressed as follows:

$$y\left(x,t\right) = \sum_{n=1}^{\infty} y_n\left(x,t\right) \tag{13}$$

In Eq. (13), $y_n\left(x,t\right)$ is the solution corresponding to β_n for n = 1, 2, 3, …, and is expressed as:

$$y_n\left(x,t\right) = X_n\left(x\right) T_n\left(t\right) \tag{14}$$

The solution of the forced vibration problem in Eq. (1) is expressed using modal superposition as follows:

$$y(x,t) = \sum_{n=1}^{\infty} X_n(x) q_n(t) \tag{15}$$

In Eq. (15), $X_n(x)$ is the nth mode shape defined in Eq. (12) and q_n is the generalized modal coordinate that needs to be determined. Substituting Eq. (15) in Eq. (1), multiplying both sides by $X_m(x)$ and integrating both sides from 0 to l yields uncoupled ODE because of the orthogonality property of the mode shapes. The uncoupled equations are in terms of the generalized modal coordinate and can be expressed as:

$$\frac{d^2}{dt^2} q_n(t) + \omega_n^2 q_n(t) = \frac{1}{\rho A \gamma_n} Q_n(t) \tag{16}$$

In Eq. (16), $\gamma_n = \int_0^l X_n^2(x)\,dx$ and $Q_n(t) = \int_0^l X_n(x) f_s(x,t)\,dx$. Including damping in the above formulation, the uncoupled equations can be re-written as:

$$\frac{d^2}{dt^2} q_n(t) + 2\omega_n \xi_n \frac{d}{dt} q_n(t) + \omega_n^2 q_n(t) = \frac{1}{\rho A \gamma_n} Q_n(t) \tag{17}$$

Eq. (17) is analogous to Eq. (16) and ξ_n is the damping ratio corresponding to the nth equation. All other variables in Eq. (17) are identical to the variables in Eq. (16).

The number of modes that need to be controlled has to be established in order to implement the control algorithms. This paper builds the control algorithms for controlling only the first three modes of the beam. This, however, does not limit or constrain the development of the control algorithm in any way.

For sinusoidal excitation acting along the length of the beam at x_s, modeled as a point load, the input load can be expressed as:

$$f_s(x,t) = f_0 Sin\omega t\, \delta(x - x_s) \tag{18}$$

In Eq. (18), f_0 is the amplitude of the sinusoidal point load per unit length of the beam, ω is the excitation frequency and δ (.) is the impulse function used for expressing the point load. Substituting Eq. (18) in $Q_n(t)$ yields:

$$Q_n(t) = f_0 Sin\omega t\, X_n(x_s) \tag{19}$$

Substituting $Q_n(t)$ from Eq. (19) in Eq. (17), yields the uncoupled equations in terms of the generalized modal coordinates as:

$$\ddot{q}_n(t) + 2\omega_n \xi_n \dot{q}_n(t) + \omega_n^2 q_n(t) = \frac{f_0}{\rho A \gamma_n} Sin\omega t\, X_n(x_s) \tag{20}$$

The steady-state solution of Eq. (20) can be simplified to the following form:

$$q_n(t) = \frac{f_0}{\rho A \gamma_n \omega_{d,n}} X_n(x_s) \int_0^t e^{-\xi_n \omega_n \tau} Sin\omega_{d,n}\tau \; Sin\omega(t-\tau)\, d\tau \qquad (21)$$

In Eq. (21), $\omega_{d,n}$ is the damped frequency. Using Eqs. (15) and (21), and using only the first three modes, the overall steady-state displacement of the cracked beam due to the sinusoidal, point load excitation input can be expressed as follows:

$$\begin{aligned} y(x,t) = {} & \frac{f_0}{\rho A \gamma_1} X_1(x) X_1(x_s) \int_0^t \frac{e^{-\xi_1 \omega_1 \tau}}{\omega_{d,1}} Sin\,\omega_{d,1}\tau \; Sin\omega(t-\tau)\, d\tau \\ & + \frac{f_0}{\rho A \gamma_2} X_2(x) X_2(x_s) \int_0^t \frac{e^{-\xi_2 \omega_2 \tau}}{\omega_{d,2}} Sin\,\omega_{d,2}\tau \; Sin\omega(t-\tau)\, d\tau \\ & + \frac{f_0}{\rho A \gamma_3} X_3(x) X_3(x_s) \int_0^t \frac{e^{-\xi_3 \omega_3 \tau}}{\omega_{d,3}} Sin\,\omega_{d,3}\tau \; Sin\omega(t-\tau)\, d\tau \end{aligned} \qquad (22)$$

In Eq. (22), $X_i(x)$ and $X_i(x_s)$ can be substituted from Eq. (12).

This yields the steady-state solution for a cantilever beam with a transverse crack located anywhere along the length of the beam that is excited by a sinusoidal point load. The model developed in this section will be used in the subsequent section to build control algorithms in order to reduce displacement at specific points on the beam or over a certain length of the beam in order to mitigate crack propagation.

3. Control Algorithms

This section presents two feed-forward control algorithms in order to reduce or minimize transverse displacement of the cracked cantilever beam by using the model developed in the previous section.

Applying Fourier transform to the steady-state solution in Eq. (22) results in a transfer function form for the transverse displacement of the beam in the frequency domain and can be expressed as:

$$Y(x,\omega) = H_s(x,\omega)\, \mathbb{F}\left[f_0 Sin\omega t\right] \qquad (23)$$

In Eq. (23), $Y(x,\omega) = \mathbb{F}\left[y(x,t)\right]$, i.e. the Fourier transform of the transverse displacement, and $H_s(x,\omega)$ is defined as follows:

$$H_s(x,\omega) = \frac{1}{\rho A}\left[\begin{array}{l} X_1(x)\dfrac{X_1(x_s)}{\gamma_1} H_1(\omega) + X_2(x)\dfrac{X_2(x_s)}{\gamma_2} H_2(\omega) \\ + X_3(x)\dfrac{X_3(x_s)}{\gamma_3} H_3(\omega) \end{array}\right] \qquad (24)$$

It may be noted that the three terms in Eq. (24) correspond to the three modes that are being used, the number of terms will increase as the number of modes for computing the steady-state solution is increased. In Eq. (24), $H_1(\omega)$, $H_2(\omega)$ and $H_3(\omega)$ are defined as:

$$H_n(\omega) = \frac{1}{\omega_n^2 - \omega^2 + 2j\omega\omega_n\xi_n} \tag{25}$$

In Eq. (25), n = 1, 2, 3 yields $H_1(\omega)$, $H_2(\omega)$ and $H_3(\omega)$, corresponding to the three modes that are being used to compute the steady-state displacement of the beam.

Eq. (23) can be re-written in the form of a transfer function as follows:

$$\frac{Y(x,\omega)}{F_s(\omega)} = H_s(x,\omega) = \frac{1}{\rho A}\sum_{n=1}^{3} X_n(x)\frac{X_n(x_s)}{\gamma_n}H_n(\omega) \tag{26}$$

In Eq. (26), $F_s(\omega) = \mathbb{F}[f_0 Sin\omega t]$, i.e. the Fourier transform of the input excitation. Eq. (26) yields the transfer function between the transverse deflection of the cracked beam and the input excitation due to a sinusoidal point load with a known excitation frequency.

For an additional point load acting along the length of the beam, due to the control force of a feed-forward controller, the transverse displacement can be expressed by superposition as:

$$Y(x,\omega) = H_s(x,\omega)F_s(\omega) + H_c(x,\omega)F_c(\omega) \tag{27}$$

In Eq. (27), $F_c(\omega)$ is the Fourier transform of the time-varying control force and $H_c(x,\omega)$ is the transfer function between the transverse displacement and the control force, and is defined as follows:

$$H_c(x,\omega) = \frac{1}{\rho A}\sum_{n=1}^{3} X_n(x)\frac{X_n(x_c)}{\gamma_n}H_n(\omega) \tag{28}$$

In Eq. (28), x_c is the location of the control force, also acting as a point load. X_n, γ_n and H_n are the same as previously defined. The control force, $F_c(\omega)$, is defined as follows:

$$F_c(\omega) = H(\omega)F_s(\omega) \tag{29}$$

In Eq. (29), $H(\omega)$ is the Fourier transform of the impulse response of the controller. Eq. (29) is expressed in time domain as follows:

$$f_c(t) = \int_{-\infty}^{\infty} h(\tau) f_s(t-\tau) d\tau \tag{30}$$

In Eq. (30), $h(\tau)$ is the impulse response of the controller that needs to be determined for a control force acting at point x_c along the length of the beam. It may be noted that the controller defined in Eq. (30) is non-causal, meaning that the future values of the excitation input are assumed to be known. Since the controller is being developed for a known disturbance acting as a sinusoidal input, the excitation load is predictable and is assumed to be known a priori.

The main objective for introducing a feed-forward control force in this paper is to minimize transverse displacement at the crack location, thereby mitigating crack propagation. Two control algorithms are introduced to meet this objective. The first algorithm minimizes the displacement at the crack location, therefore yielding the following condition:

$$Y(x,\omega)\Big|_{x=l_1} = 0 \Rightarrow H(\omega) = -\frac{H_s(l_1,\omega)}{H_c(l_1,\omega)} \tag{31}$$

Eq. (31) results from the substitution of Eq. (29) in Eq. (27) for the crack location $x = l_1$ and enforcing the resulting displacement at the crack location to be zero. This yields the control law and can be used to compute the required control force as:

$$f_c(t) = \mathbb{F}^{-1}\left[F_c(\omega)\right] = \mathbb{F}^{-1}\left[H(\omega)F_s(\omega)\right] = \mathbb{F}^{-1}\left[-\frac{H_s(l_1,\omega)F_s(\omega)}{H_c(l_1,\omega)}\right] \tag{32}$$

In Eq. (32), $\mathbb{F}^{-1}$ is the inverse Fourier transform and f_c is the control force per unit length of the beam that satisfies the control requirement expressed in Eq. (31).

The second control algorithm is based on minimizing the transverse displacement over a certain length of the beam that contains the crack. The control objective is defined as the minimization of the mean square value of transverse displacement of the beam over a specific length of the beam. Solving for the control objective yields the following form of $H(\omega)$ [6]:

$$H(\omega) = \frac{-\int_{x_1}^{x_2} H_s(x,\omega)H_c^*(x,\omega)dx}{\int_{x_1}^{x_2}\left|H_c(x,\omega)\right|^2 dx} \tag{33}$$

In Eq. (33), H_c^* is the complex conjugate of H_c, defined in Eq. (28) and x_1 and x_2 are the lower bound and the upper bound of the beam length over which the transverse displacement is being minimized. The corresponding control force resulting from the outcome in Eq. (33) is as follows:

$$f_c(t) = \mathbb{F}^{-1}\left[F_c(\omega)\right] = \mathbb{F}^{-1}\left[H(\omega)F_s(\omega)\right]$$
$$= \mathbb{F}^{-1}\left[\frac{-\int_{x_1}^{x_2} H_s(x,\omega)H_c^*(x,\omega)dx}{\int_{x_1}^{x_2}\left|H_c(x,\omega)\right|^2 dx}F_s(\omega)\right] \quad (34)$$

The control forces derived in Eqs. (32) and (34), therefore, yield the results for the governing algorithms in order to eliminate transverse displacement at the crack location or minimize transverse displacement over a length of the beam that includes the crack, when the beam is excited by a known point load sinusoidal disturbance input. The subsequent section will use the control algorithms developed in this section for a simulation in order to demonstrate the effectiveness of the control algorithms in reducing transverse displacements as well as reducing the rate of crack propagation of the damaged beam, and increasing its useful life.

4. Results

This section discusses the simulation results obtained by using the formulation presented in Sections 2 and 3. The simulation is used to demonstrate the differences between the controlled and un-controlled response and the effectiveness of the proposed feed-forward control algorithms.

The dimensions of the cantilever beam used for simulation are as follows: 600 *mm* (*l*) × 30 *mm* (*b*) × 15 *mm* (*h*). The beam is made of 7075-T651 Aluminum, a density of 2700 kg/m^3 and a modulus of elasticity of 70 *GPa* are used as the material properties of the beam. The first three frequencies of the above specified un-cracked cantilever beam are computed to be 34.3, 214.8 and 601.4 *Hz*. The corresponding damping ratios for all three modes are assumed to be 0.02, primarily due to material damping. A crack is introduced to be at l_1 = 200 *mm* from the origin of the coordinate system with a crack depth, *a*, of 1.5 *mm*. The excitation source is located at the edge of the beam, at x_s = 600 *mm* in order to maximize the bending moment acting on the crack. The excitation source is placed such that it does not coincide with any of the nodes for the first three natural modes of the cantilever beam which are located at 302 *mm*, 470 *mm* and 520 *mm* from the origin.

Fig. 2(a) shows the simulated magnitude response of the uncontrolled beam, when excited by a sinusoidal load with an amplitude of 1 *N/m* and an excitation frequency that is identical to the first natural frequency of the beam. The controlled response is simulated by placing the controller at x_c = 400 *mm* and

the control algorithm that minimizes deflection at the crack location is used for the controlled response shown in Fig. 2(b).

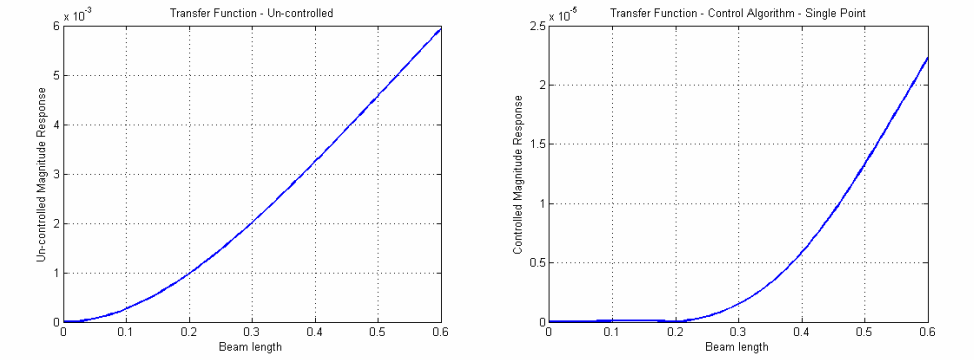

(a) (b)

Fig. 2. Beam Response – Excitation at First Mode (a) Un-controlled (b) Controlled

As can be seen from the comparison of Figs. 2(a) and 2(b), the magnitude response reduces by orders of magnitude with even more significant reduction around the crack location ($x = l_1 = 0.2$). Figs. 3(a) and 3(b) show another two simulation results to compare the uncontrolled and controlled response when the excitation frequency is between first and second natural frequency, and when the excitation frequency coincides with the second natural frequency respectively.

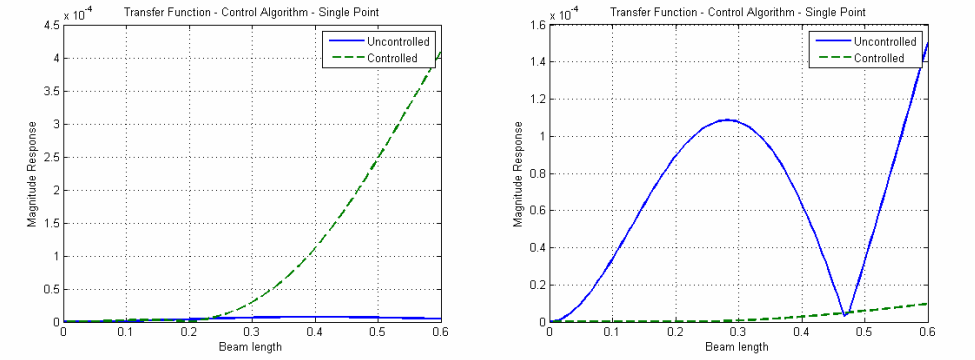

(a) (b)

Fig. 3. Beam Response (a) Excitation between First & Second Modes (b) Excitation at Second Mode

It can be concluded from the simulated responses in Figs. 2 and 3 that the magnitude responses over the entire length of the beam are substantially reduced when the excitation frequency coincides with a natural frequency of the beam. However, the displacement amplitude does not change appreciably over the entire length when the excitation frequency does not coincide with a natural frequency, as seen in Fig. 3(a). This can be attributed to the fact that only one control actuator is being used, resulting in poor performance when excitation is governed by more than one natural mode of the beam. The best controlled response is achieved when

the beam response is dominated by one mode only. The three plots can be further used to conclude that the crack propagation will be significantly mitigated if the excitation frequency is such that the beam response is dominated by a single mode, and it may further be concluded that the rate of crack propagation may not change significantly if more than one natural mode is being excited by the disturbance input. Fig. 4 shows a comparison between the excitation force and the control force that corresponds to the controlled response shown in Fig. 2(b). It may be noted that the control effort can be significantly reduced if the controller is co-located at the location of the excitation input.

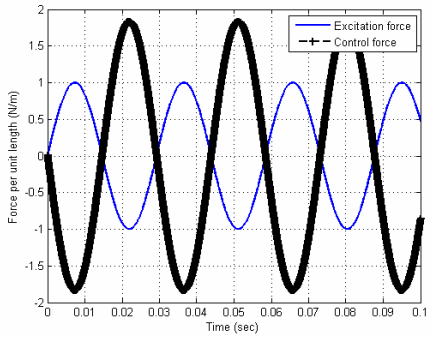

Fig. 4. Excitation versus control force – Excitation at First Mode

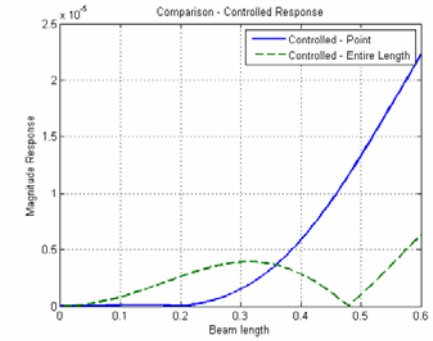

Fig. 5. Controlled Response – Excitation at First Mode

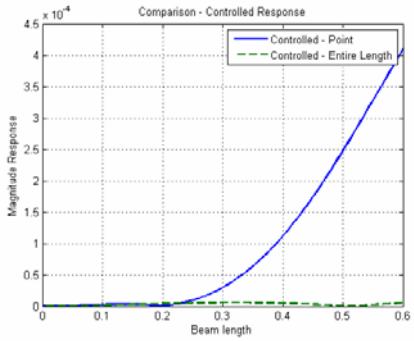

Fig. 6. Controlled Response – Excitation between First & Second Modes

Figs. 5 and 6 compare the controlled response between the two feed-forward control algorithms outlined in the previous section. Fig. 7 demonstrates the sensitivity of the response amplitude to the placement of the controller actuator when the disturbance input excites the first mode only. Co-location of the controller actuator with the excitation input, if possible, results in minimum amplitudes. This can be observed in Fig. 7 for the controller location of 0.6 *m* (600 *mm*), which is coincident with the excitation location for this simulation. However, placement of the controller at a location that coincides with a node will result in significant deterioration of the control performance.

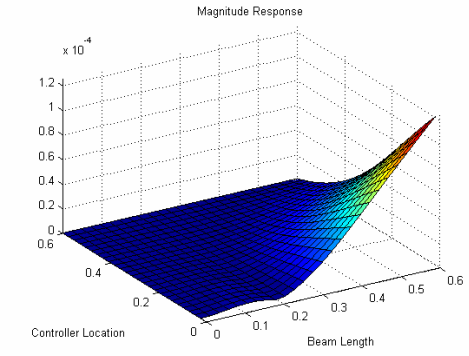

Fig. 7. Varying Controller Location

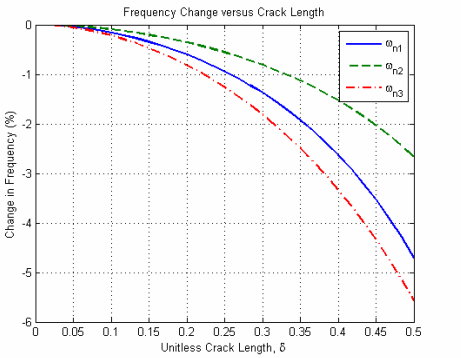

Fig. 8. Natural Frequency v/s Crack Length

Another simulation run is performed in order to determine the influence of the proposed control algorithms on the useful life of the cantilever beam with a pre-existing crack depth of 1.5 *mm*. A sinusoidal load varying between 720 *N* and 240 *N* is used as the excitation input at x_s = 600 *mm*, resulting in maximum and minimum normal stresses of 128 *MPa* and 42.7 *MPa* respectively, and the excitation frequency of the input load is 10 *Hz*. All other parameters remain the same as in the previous simulation. Using linear elastic fracture mechanics (LEFM), the crack depth is expected to extend till 7.5 *mm* before failure due to brittle fracture can be expected. Fig. 8 shows the drop in natural frequencies resulting from crack propagation, as the crack length increases from 1.5 *mm* to 7.5 *mm*. The controlled response is simulated by placing the controller at x_c = 400 *mm* and the control algorithm that minimizes deflection at the crack location is used to determine the control force. The useful life of the beam is computed as the number of cycles it takes the crack to propagate from 1.5 *mm* to 7.5 *mm*, using modified Paris law and numerical integration [18, 19] and is briefly discussed in Appendix B.

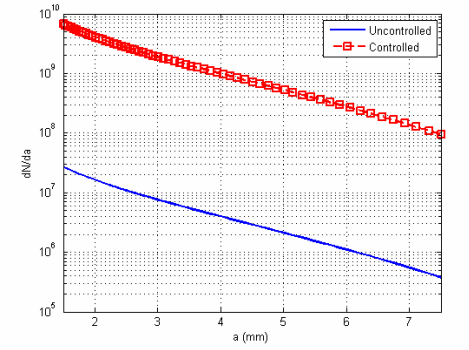

Fig. 9. Crack Propagation Results

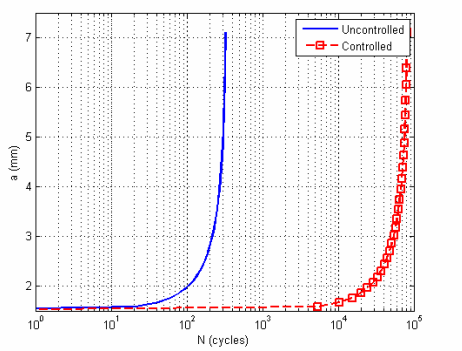

Fig. 10. a-N Plot – Comparison

The results are shown in Fig. 9 with the area under the curve representing useful life. As can be observed from Fig. 9, implementation of the control algorithm results in increasing useful life by an order of magnitude. Fig. 10 shows the a-N plot comparing crack growth between the un-controlled and the controlled beam, an order of magnitude increase in the useful life can be observed from this plot as well. This serves as a validation of the proposed control algorithms to minimize transverse deflection of the damaged beam and simultaneously reduce the rate of crack propagation and, hence, increase the useful life of the damaged beam.

5. Conclusions

This paper proposes the use of two feed-forward control algorithms in order to minimize transverse deflection as well as mitigate crack propagation in a cantilever beam with a pre-existing single-sided open-crack. Simulation results demonstrate that transverse displacement is substantially reduced when the beam response is dominated by a single mode, and that the useful life of the damaged beam can be increased by an order of magnitude. The results further demonstrate that the control effort can be minimized if the controller is co-located with the excitation source.

The control algorithms presented in this paper can be used in conjunction with crack detection and identification techniques by studying changes in natural frequencies and mode shapes or by the analysis of the vibration response of the beam, and thereby identifying the crack size and the crack location. Once the crack is detected, one of the two control algorithms presented in this paper can be used to significantly reduce the rate of crack propagation and enhance the useful life of the damaged structure. Future work will implement the proposed algorithms on breathing cracks. Future work will also be undertaken to implement the proposed algorithms on truss structures and experimentally evaluate the implementation of the feed-forward algorithms proposed in this paper by using a semi-active control device so as to minimize power requirements.

R E F E R E N C E S

[1]. *G. W. Housner*, *L. A. Bergman*, *T. K. Caughey*, *A. G. Chassiakos*, *R. O. Claus*, *S. F. Masri*, *R. E. Skelton*, *T. T. Soong*, *B. F. Spencer*, *J. T. P. Yao*, "Structural Control: Past, Present, and Future", ASCE Journal of Engineering Mechanics, **vol. 123**, no. 9, 1997, pp. 897-971.

[2]. *R. Alkhatib*, *M. F. Golnaraghi*, "Active Structural Vibration Control: A Review", The Shock and Vibration Digest, **vol. 35**, no. 5, 2003, pp. 367-383.

[3]. *L. Meirovitch*, Dynamics and Control of Structures, John Wiley & Sons, New York, USA, 1990.

[4]. *T. T. Soong*, Active Structural Control: Theory and Practice, Longman Scientific & Technical, UK, 1990.

[5]. *C. R. Fuller*, *S. J. Elliott*, *P. A. Nelson*, Active Control of Vibration, Academic Press, London, UK, 1997.
[6]. *J. T. Post*, Active Control of the Forced and Transient Response of a Finite Beam, NASA-CR-181957, NASA, USA, 1990.
[7]. *A. D. Dimarogonas*, "Vibration of Cracked Structures: A State of the Art Review", Engineering Fracture Mechanics, **vol. 55**, no. 5, 1996, pp. 831-857.
[8]. *O. S. Salawu*, "Detection of Structural Damage through Changes in Frequency: A Review", Engineering Structures, **vol. 19**, no. 9, 1997, pp. 718-723.
[9]. *Y. Shih*, *G. Wu*, "Effect of Vibration on Fatigue Crack Growth of an Edge Crack for a Rectangular Plate", International Journal of Fatigue, **vol. 24**, 2002, pp. 557-566.
[10]. *A. C. Chasalevris*, *C. A. Papadopoulos*, "Identification of Multiple Cracks in Beams under Bending", Mechanical Systems and Signal Processing, **vol. 20**, 2006, pp. 1631-1673.
[11]. *U. Lee*, *J. Shin*, "A Frequency Response Function-based Structural Damage Identification Method", Computers and Structures, **vol. 80**, 2002, pp. 117-132.
[12]. *J. Lee*, "Identification of a Crack in a Beam by the Boundary Element Method", Journal of Mechanical Science and Technology, **vol. 24**, no. 3, 2010, pp. 801-804.
[13]. *T. G. Chondros*, *A. D. Dimarogonas*, *J. Yao*, "A Continuous Cracked Beam Vibration Theory", Journal of Sound and Vibration, **vol. 215**, no. 1, 1998, pp. 17-34.
[14]. *S. M. Cheng*, *X. J. Wu*, *W. Wallace*, *A. S. J. Swamidas*, "Vibration Response of a Beam with a Breathing Crack", Journal of Sound and Vibration, **vol. 225**, no. 1, 1999, pp. 201-208.
[15]. *B. S. Haisty*, *W. T. Springer*, "A General Beam Element for use in Damage Assessment of Complex Structures", ASME Journal of Vibration, Acoustics, Stress, and Reliability in Design, **vol. 110**, 1988, pp. 389-394.
[16]. *W. M. Ostachowicz*, *M. Krawczuk*, "Analysis of the Effect of Cracks on the Natural Frequencies of a Cantilever Beam", Journal of Sound and Vibration, **vol. 150**, no. 2, 1991, pp. 191-201.
[17]. *Y. Narkis*, "Identification of Crack Location in Vibrating Simply Supported Beams", Journal of Sound and Vibration, **vol. 172**, no. 4, 1994, pp. 549-558.
[18]. *N. E. Dowling*, Mechanical Behavior of Materials, 2nd Edition, Prentice Hall, New Jersey, USA, 1999.
[19]. *T. L. Anderson*, Fracture Mechanics: Fundamentals and Applications, 3rd Edition, CRC Press, Florida, USA, 2004.

APPENDIX A

The change in strain energy of the torsional spring used to model the crack, as discussed in Section 2, can be represented in terms of the bending moment, M, at the crack location as follows:

$$\Delta U = \frac{M^2}{2K_t} \tag{A.1}$$

In Eq. (A.1), ΔU is the change in strain energy and K_t is the torsional stiffness of the spring. The change in strain energy resulting from the presence of the crack can be expressed in terms of the stress intensity factor as [18, 19]:

$$\Delta U = \frac{1}{E}\int_0^A K_I^2 \, dA \tag{A.2}$$

In Eq. (A.2), K_I is the stress intensity factor (SIF) corresponding to Mode I (opening mode) of crack propagation, E is the modulus of elasticity of the beam material and A is the area of the cracked section of the beam at the crack location. Only Mode I is considered for contribution to any change in strain energy in Eq. (A.2), since shear due to bending is expected to be negligible. It may be noted that Eq. (A.2) holds for a plane stress condition only. A modified form of the modulus of elasticity can be used for plane strain applications.

The stress intensity factor corresponding to a crack length, a, and a nominal (or far-field) stress of σ is defined as follows:

$$K_I = \sigma\sqrt{\pi a}\,F(\delta) \tag{A.3}$$

In Eq. (A.3), $F(\delta)$ is a dimensionless function governed by geometry, boundary conditions and loading conditions of the cracked structure, and δ is the dimensionless crack length. For a cantilever beam with a rectangular cross-section and a bending load acting on the cross-section which results in an opening mode, the dimensionless function is empirically defined as [18, 19]:

$$F(\delta) = \frac{\sqrt{\frac{2}{\pi\delta}Tan\left(\frac{\pi\delta}{2}\right)}}{Cos\left(\frac{\pi\delta}{2}\right)}\left[0.923 + 0.199\left\{1 - Sin\left(\frac{\pi\delta}{2}\right)\right\}^4\right] \tag{A.4}$$

Substituting Eqs. (A.3) and (A.4), with $\sigma = \frac{6M}{bh^2}$ and $dA = bd\alpha$, in Eq. (A.2) and equating Eqs. (A.1) and (A.2) yields the following:

$$\frac{1}{K_t} = \frac{72\pi}{Ebh^4}\int_0^a \alpha F^2 d\alpha \tag{A.5}$$

Solving Eq. (A.5) yields the torsional stiffness of the modeled spring used to represent the crack. K_t, as defined in Eq. (A.5), represents the torsional stiffness of the spring used to model the open single sided edge-crack, as shown in Fig. 1. It may be noted that the torsional stiffness is a function of relative crack length, and, therefore, changes as the crack propagates. This modeled stiffness has been used in Sections 2 and 3 in the form of a dimensionless stiffness constant, K, defined as:

$$K = \frac{K_t l}{EI} \tag{A.6}$$

In Eq. (A.6), I is the area moment of inertia of the entire un-cracked cross-section of the beam. K is called the crack section stiffness and is dimensionless. The inverse of K, represented by θ, is called the crack section compliance or flexibility and has been used in the governing beam equation in Sections 2 and 3 to model the crack.

APPENDIX B

The rate of crack propagation in a damaged structure is most widely modeled by using the modified Paris Law, also commonly called as the Walker equation, and is expressed as:

$$\frac{da}{dN} = \frac{C_1}{\left(1-R\right)^{m_1(1-\gamma)}}\left(\Delta K\right)^{m_1} \tag{B.1}$$

In Eq. (B.1), C_1, m_1 and γ are material constants, R is the ratio between the minimum and maximum stress intensity factors that the crack geometry is subject to and ΔK is the range of the stress intensity factors resulting from cyclic loading.

For constant amplitude loading, the Walker equation is expressed iteratively so as to compute crack growth per unit cycle or vice versa. This is written as:

$$\left(\frac{dN}{da}\right)_j = \frac{1}{C\left(\Delta K_j\right)^m} = \frac{1}{C\left(F_j \Delta S\sqrt{\pi a_j}\right)^m} \tag{B.2}$$

In Eq. (B.2), ΔS is the stress range and F_j is the dimensionless function of crack length, defined in Appendix A, Eq. (A.4), for the geometry and boundary conditions of the cantilever beam used in this paper. Furthermore, C is used to replace the coefficient in Eq. (B.1) and is a function of the material constants and the ratio, R.

The Walker equation can be used to compute the number of loading cycles that will lead to final failure as the crack propagates. Using the modified Simpson's rule, life of the damaged structure can be computed as [18]:

$$N_{if} = \sum_j \frac{a_j\left(r^2-1\right)}{6r}\left[\left(\frac{dN}{da}\right)_j r\left(2-r\right)+\left(\frac{dN}{da}\right)_{j+1}\left(r+1\right)^2+\left(\frac{dN}{da}\right)_{j+2}\left(2r-1\right)\right] \tag{B.3}$$

In Eq. (B.3), N_{if} is the number of cycles that the crack takes to propagate from length a_i to length a_f and r is the increment in crack length used for integration such that $a_f = r^n a_i$ and n is any even number, with the substitution of Eq. (B.2). A value of r = 1.0272 and n = 60 has been used for calculating N_{if} in the simulation presented in Section 4 with a_i = 1.5 *mm* and a_f = 7.5 *mm*. The material constants used for computing N_{if} in the simulation in Section 4 are $C_1 = 2.71\times10^{-11}$ $\frac{m/cycle}{\left(MPa\sqrt{m}\right)^{m_1}}$, m_1 = 3.7 and γ = 0.641.